Microtechnique: 2023-2024 Master Semester 1
Fundamentals of integrated photonic components

Solution for Assignment #5
Multi mode interferometer (MMI)

Problem 1: Multimode waveguide (25 points)

Consider the step-index multimode waveguide in Fig.1.

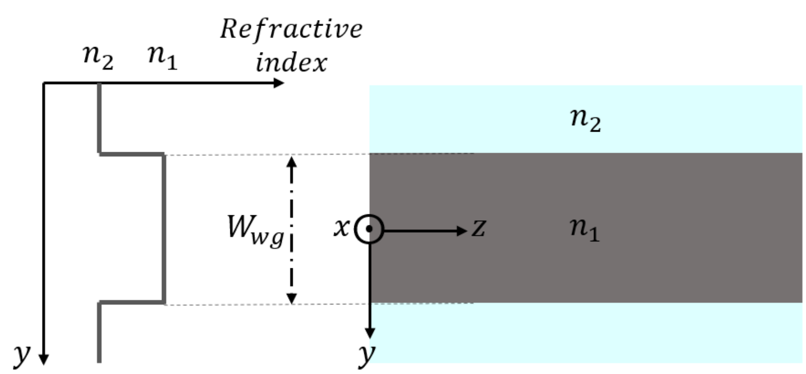

Figure 1: 2D representation of a step-index multi-mode waveguide: refractive index profile (left), and top view of ridge boundaries and coordinate system (right).

a) Derive the expression for the beat length of the two lowest order modes (m = 0 and m = 1) and calculate its value. **(10 points)**

b) Create a model of a Lithium Niobate slab waveguide (n_1 = 2.1376) embedded in SiO_2 (n_2 = 1.45), as depicted in Figure 2, with the following parameters:
$l_{wg} = l_{SiO2} = 1\ \mu m$
$w_{wg} = 4\ \mu m$
$t_{wg} = 0.3\ \mu m$
$t_{SiO2} = 1.3\ \mu m$
$w_{SiO2} = 6\ \mu m$
Choose a simulation range in wavelength between 1.5 μm and 1.6 μm. Create a 3-modes port at the input of the waveguide and provide the refractive index of the first three modes around 1.55 μm **(5 points)**

c) From the refractive index values in the CST simulation, calculate the beat length between the first two modes. Compare the value to the one from the analytical formula discussed in class and obtained in point (a). **(5**

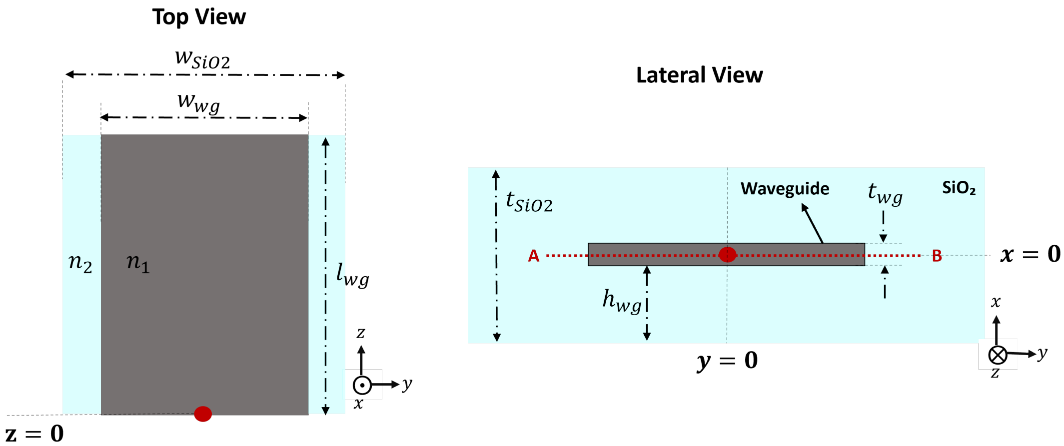

Figure 2: 2D representation of the Si-Slab waveguide.

points)

d) Calculate the beat length between the zeroth and second modes **(5 points)**

Solution:

a) Consider a simple step-index multimode waveguide with the width W_{wg}, ridge refractive index $n_1 = n_{eff}$ and cladding refractive index n_2. The waveguide supports a number of k modes with orders $m = 0, 1, ..., k-1$ at wavelength λ_0. We also assume that the waveguide exhibits a high refractive index contrast, i.e., $n_1 \gg n_2$. This implies that we can approximate the effective refractive indices of the waveguide modes with that of the core, i.e., $n^m_{eff} \approx n_1$. In this case, the dispersion relation governing this waveguide can be expressed as:

$$k^2_{ym} + \beta^2_m = k^2_0 n^2_1 \tag{1}$$

where $k_0 = \dfrac{2\pi}{\lambda_0}$ and $k_{ym} = \dfrac{(m+1)\pi}{W_m}$. W_m is the effective width of the m^{th} mode along y-axis. Similarly to the effective refractive indices, in high-contrast waveguides, the widths W_m associated with each mode can be all considered having the same size, being expressed for TE mode as

$$W_{TEm} = W_{wg} + \left(\frac{\lambda_0}{\pi}\right)\frac{1}{\sqrt{n^2_1 - n^2_2}} \approx W_0 \tag{2}$$

being the second contribution negligible compared to W_{wg}. Now, by applying a binomial expansion and assuming $k^2_{ym} \ll k^2_0 n^2_{eff}$ (as $W_m \gg \lambda_0$), derived from the dispersion equation 1, the propagation constant can be written as

$$\beta_m \approx k_0 n_r - \frac{(m+1)^2 \pi \lambda_0}{4 n_1 W^2_0} \tag{3}$$

From Eq. 3, we note that the propagating constant has a quadratic dependence upon the **mode number m**. Now, **beat length of the two lowest order modes**, L_π, can be written as

$$L_\pi = \frac{\pi}{\beta_0 - \beta_1} = \frac{\pi}{\Delta\beta} \approx \frac{4 n_1 W^2_0}{3\lambda_0} \tag{4}$$

Therefore, we can use the last part of Eq. 4 to calculate the beat length of the two lowest-order modes based on the geometrical properties of our waveguides. Once the beat length is known, we can reuse 4 and easily derive the propagating constant spacing $\Delta\beta$ as:

$$\Delta\beta = \beta_0 - \beta_m \approx \frac{m\,(m+2)\,\pi}{3L_\pi} \tag{5}$$

b) The simulations of the multimode waveguide provide the following values $n^0_{eff} = 1.773$ $n^1_{eff} = 1.74426$, and $n^2_{eff} = 1.696$

c) Plugging n^0_{eff} and n^1_{eff} into the general definition of the beat length, we obtain the following:

$$L_\pi = \frac{\pi}{\beta_0 - \beta_1} = \frac{\pi}{k_0(n^0_{eff} - n^1_{eff})} = \frac{\lambda_0}{2(n^0_{eff} - n^1_{eff})} = 27\ \mu m \tag{6}$$

while using Equation 4 we get

$$L_\pi = \frac{4n_1 W_0^2}{3\lambda_0} = \frac{4 \times 2.1376 \times 4^2}{3 \times 1.55} = 29.4\ \mu m \tag{7}$$

Therefore, the analytical model can give the beat length of the structure in first approximation.

d) Similar to previous questions, we use the equation

$$L_\pi = \frac{\pi}{\beta_0 - \beta_2} = \frac{\pi}{k_0(n^0_{eff} - n^2_{eff})} = \frac{\lambda_0}{2(n^0_{eff} - n^2_{eff})} = 10.06\ \mu m \tag{8}$$

Problem 2: Y-coupler   (40 points)

Consider the 3-port system in Figure 3. This device is known as Y-coupler. The goal is to excite the fundamental mode of port in 1 of the Y-coupler and split the input power in two, obtaining the fundamental mode at port out 2 and port out 3.

a) The central portion of the Y-coupler has length of 10 μm, behaving as a Multi-mode interferometer (MMI).

- Show the 2D profile (y component) of the zeroth and second order modes of the MMI. **(5 points)**
- Using the "Field at arbitrary coordinate" in the Post processing menu, extract the electric field (y component) of these two modes along the cut-line AB in Fig. 2 in **Problem 2 (5 points)**

b) Assuming now these two modes interfere constructively in the center of the waveguide ($(x, y) = (0, 0)$) at the input of the MMI, calculate at which distance (along z) they will cause the power splitting. **(5 points)**

We will now demonstrate how the Y-coupler works, using the length we have just calculated. Given the following parameters in Figure 3, simulate the Y-Coupler in CST.
$l_{wg} = 1.2\ \mu m$
$w_{wg} = 1.5\ \mu m$
$t_{wg} = 0.3\ \mu m$
$w_{coupler} = 4\ \mu m$
$l_{coupler} = 10\ \mu m$
$w_{sub} = 5\ \mu m$

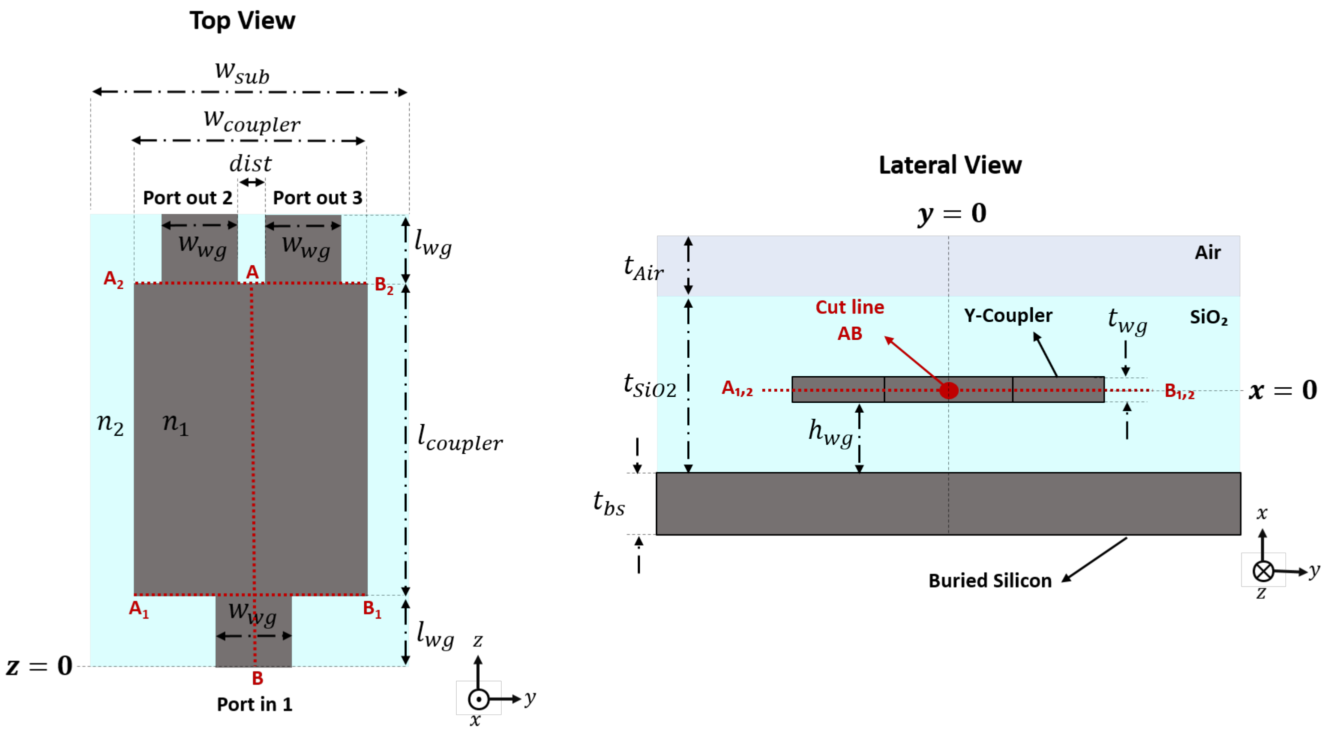

Figure 3: Top view and lateral view of the Y-coupler.

$t_{SiO2} = 1.3\ \mu m$
$t_{Air} = t_{bs} = 0.5\ \mu m$
$n_1 = 2.1376$
$n_2 = 1.45$
$dist = 0.5\ \mu m$
Use the simulation instructions as before. Consider the following additional hints:

- Choose the frequency range to be 186 THz to 200 THz and time domain simulation.
- Place an E-field monitor at $f_0 = 193.4\ THz$ (i.e., $\lambda_0 = 1.55\ \mu m$).
- Place 3 (single-mode) ports for input and outputs and restrict them around the waveguides (leaving at least 200-300 nm in every direction around them and avoiding an overlap between the ones in output).

c) Excite the fundamental mode in Port 1. For 2D plots, place also the color bar on the field intensities (keep the color-bar the same for the various questions belowe).
In order to define the cut-lines:

- For AB cut-line (See Figure 3), along z and at the center of the structure, enter the coordinates as $(x, y)_{AB} = (0, 0)$. For A_1B_1 cut line, enter the coordinates as $(x, z)_{A_1B_1} = \left(0, l_{wg}\right)$. For A_2B_2 cut line, enter the coordinates as $(x, z)_{A_2B_2} = \left(0, l_{wg} + l_{coupler}\right)$.
- Click **ok** and then **Evaluate** for each cut-line, separately.

- Show the top view of the electric field (y component, plane X = 0) **(5 points)**.
- Show the S-parameter S11, S21 and S31. Comment on the results **(5 points)**
- Show the absolute value of the electric field on the cut-line AB and comment **(5 points)**.
- Show the absolute value of the electric field on the cut-line A1B1 and comment **(5 points)**.
- Show the absolute value of the electric field on the cut-line A2B2 and comment **(5 points)**.

Solution:

a) The profiles of the fundamental and second order modes (y component, in phase) of the 4 μm waveguide are the following:

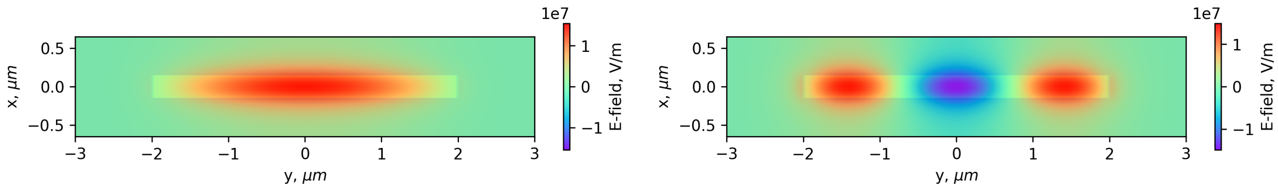

Figure 4: Zeroth and second order modes of the multimode waveguide.

The fundamental mode presents a single maximum at the center of the waveguide, while the second one has a total of three lobes and two nodes, with a central minimum and two lateral maxima. We can notice that both modes have a maximum (or a minimum) in the center of the waveguide and - reminding that a maximum can become a minimum with a phase shift of π - this property is fundamental for their excitation in the MMI: also the input mode from port 1 is, indeed, maximum for $y = 0$ and, therefore, its spatial overlap with the modes in Fig. 4 is strong at the input of the multimode waveguide. In contrast, the first order mode of the MMI presents a node in the center. As a consequence, the input efficiently excites only fundamental and second order modes, the latter with a phase shift of π.

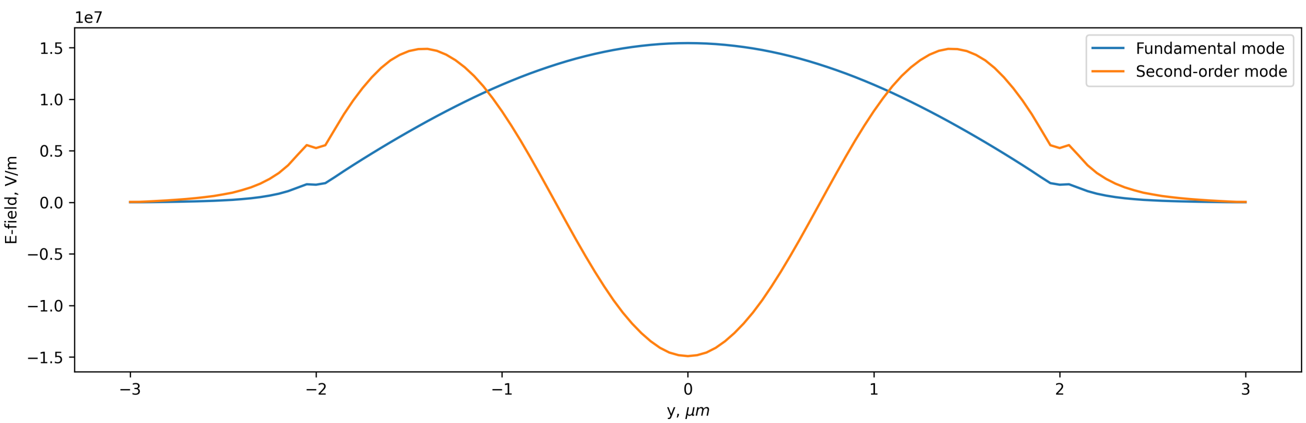

Figure 5: Fundamental and second-order modes of the MMI along the cutline AB.

We can observe that when the modes are in phase, their superposition results in a destructive interference in the center, while the lateral portions interact constructively. Therefore, if we assume an equal absolute value of the modes for $y = 0$, we obtain a central node and two lateral maxima. This result can be exploited for our Y-coupler: if we manage to efficiently excite only these two modes in the MMI and let them beat until their phase is equal, we can place the output ports in correspondence of the two maxima in Fig. 5. In this way we will excite their fundamental modes, splitting the input power in two equal components.

b) As discussed in the previous point, the two modes are both excited with a maximum in the center of the waveguide and interact constructively in this region. As a consequence, they are out of phase by a factor π. In order to obtain the power splitting, we need instead the modes in phase, with a central destructive interference. Since we know that the modes travel at a different velocity along the waveguide - beating in the process -, we can compute the length after which they accumulate another phase delay of π. This is exactly the definition of the beat length between the modes, which can therefore be calculated as

$$L_{\pi 02} = \frac{\pi}{\beta_0 - \beta_2} = \frac{\pi}{k_0(n^0_{eff} - n^2_{eff})} = \frac{\lambda_0}{2(n^0_{eff} - n^2_{eff})} = 10.06\ \mu m \tag{9}$$

c) The top view of the electric field (y component) is shown in Fig. 7

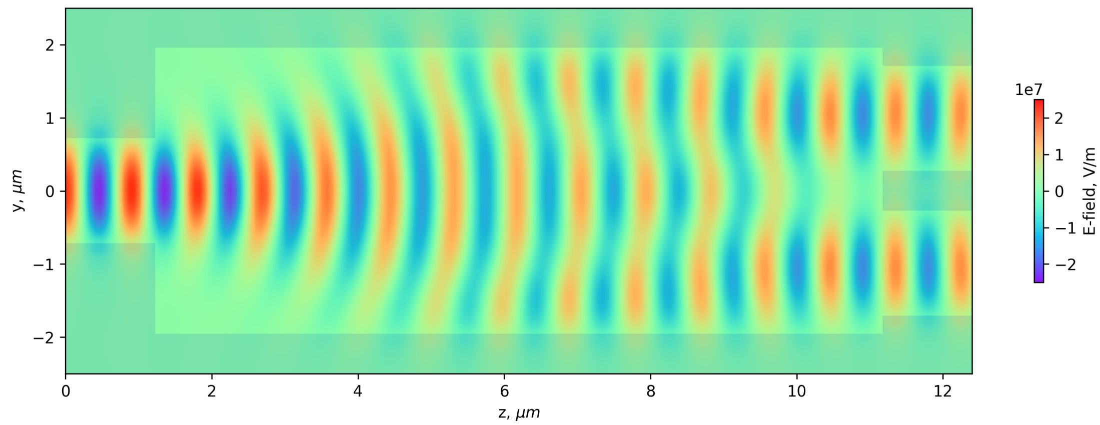

Figure 6: Y-component of electric-field viewed from the top.

Next, we extract the S-parameters as shown in

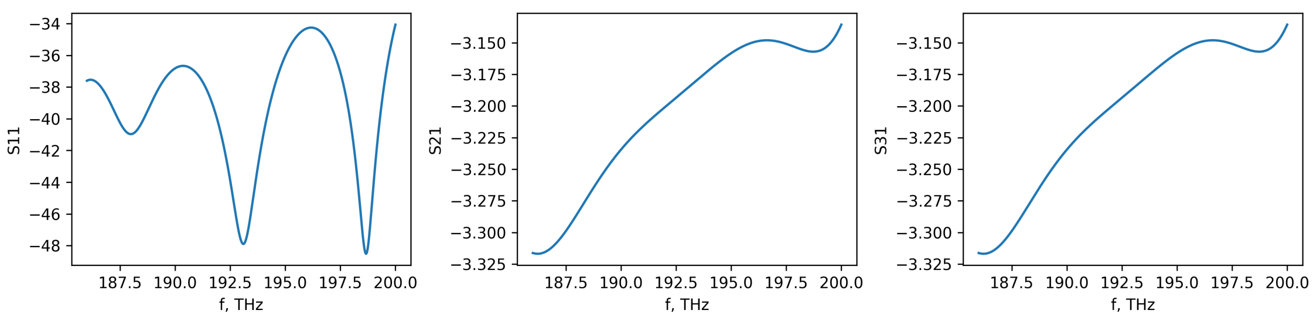

Figure 7: S-parameters where excitation is launched from port 3.

We can observe that the values of S31 and S21 are exactly the same for the full range of frequency we have analysed. Therefore, we can conclude that the input power is efficiently split in two equal components. The much lower values of S11 are a confirmation that only a negligible portion of the input is reflected back and, therefore, lost.

Finally, we extract the aboslute values of the electric field at the various ports. The results are shown in Fig. 9

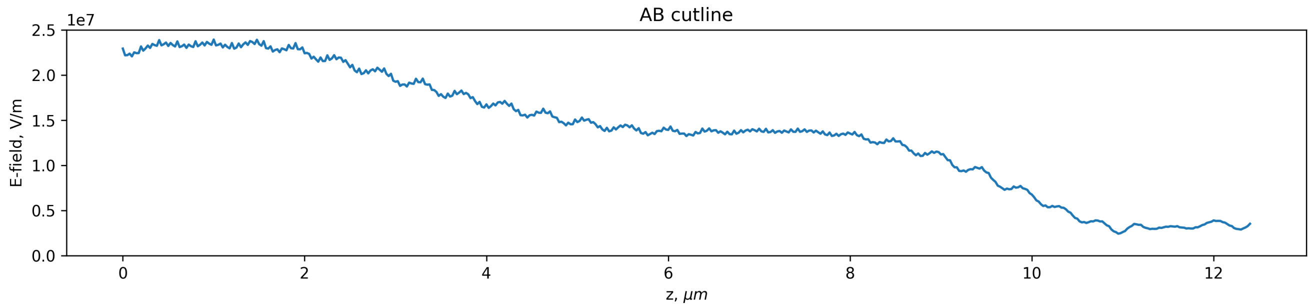

Figure 8: AB cutline for the electric-field (abs)

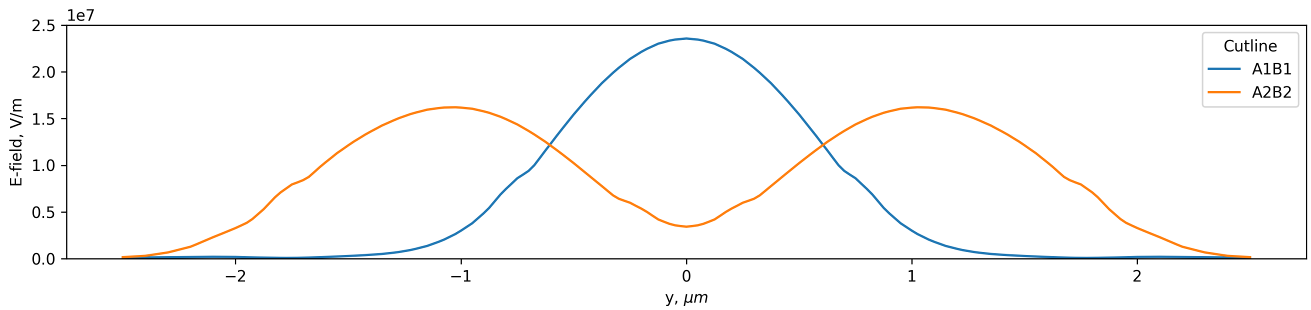

Figure 9: Cutlines for the electric-field (abs) at the ports

Problem 3: X-coupler (35 points)

Consider the 4-port system depicted here in Figure 10: this structure is another MMI known as an X-coupler. In this exercise, the proper location of the output ports is unknown (represented by the transparent output ports in Fig. 10). The correct position of the ports depends on the phase of the excited modes in the input ports.

Given the following parameters (referred to Fig. 10), create the geometry of the X-coupler in CST:
$l_{wg} = 1.2\ \mu m$
$w_{wg} = 1.5\ \mu m$
$t_{wg} = 0.3\ \mu m$
$w_{coupler} = 4\ \mu m$
$l_{coupler} = 40\ \mu m$
$w_{sub} = 6\ \mu m$
$t_{SiO2} = 1.3\ \mu m$
$t_{Air} = t_{bs} = 0.5\ \mu m$
$n_1 = 2.1376$
$n_c = 1.45$
$dist = 0.5\ \mu m$

Note: In the General properties of the mesh, set both the Cells per wavelength and the Cells per max model box edge to 6 "Near to model" and 2 "Far from model". This step will reduce the accuracy of our simulation but will greatly reduce the computational time. With these settings, CST should generate around 1 million cells.
Use the simulation instructions given for Problem 2, this time with two input and one output ports.

To define the cut-lines, follow the same procedure as before, using the following coordinates:
$(x, y)_{AB} = \left(0, -dist/2 - w_{wg}/2\right)$.

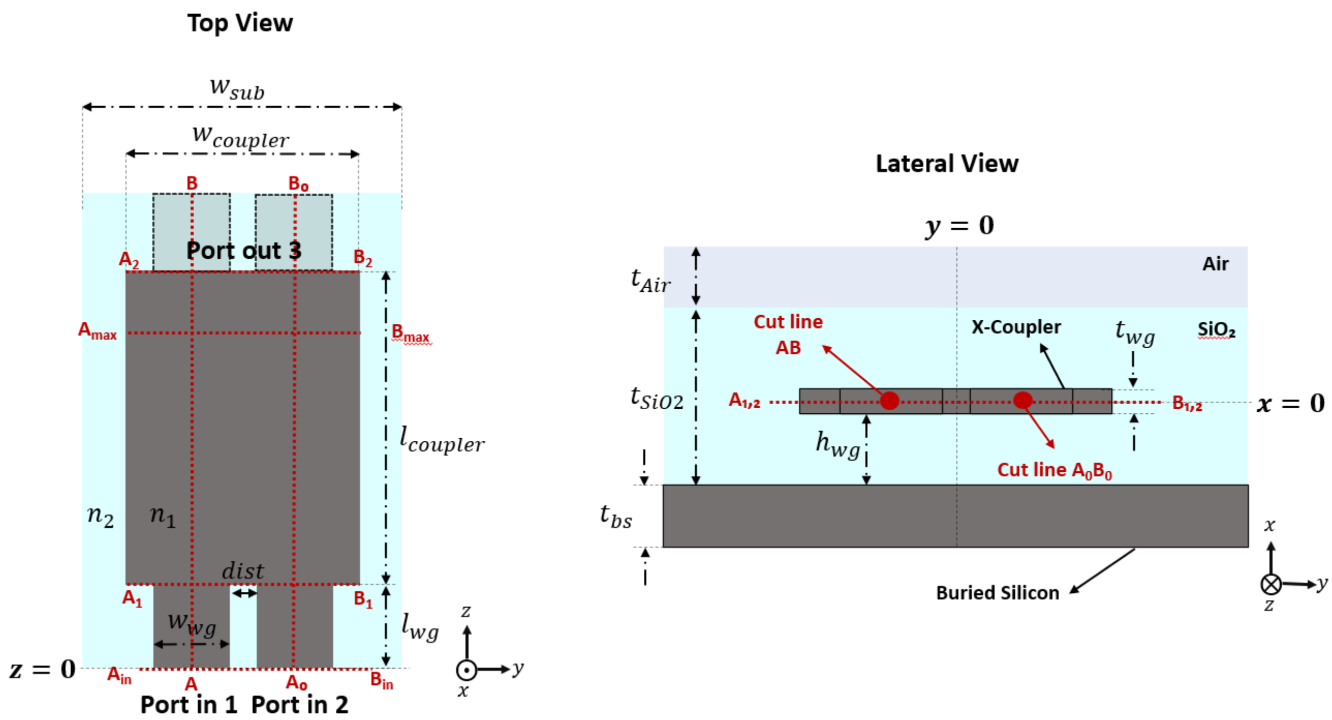

Figure 10: Top view and lateral view of the X-coupler and the cut lines of interest.

$(x, y)_{A_0B_0} = \left(0, dist/2 + w_{wg}/2\right)$.
$(x, z)_{A_1B_1} = \left(0, l_{wg}\right)$.
$(x, z)_{A_2B_2} = \left(0, l_{wg} + l_{coupler}\right)$.

a) Show the top view of the electric field (y component) on the plane X = 0 when the X-coupler is excited from both input ports **(5 points)**
To excite both ports, go to the "Time Domain Solver Parameters" and choose "list" under source type. Then, choose "Excitation list" and choose the ports you need to excite.

b) Using the field at arbitrary coordinates of the Post processing menu, plot the electric field (absolute value) along the cut-lines AB and A_0B_0 for the simulated excitation (in-phase X-Coupler). Combining these profiles with the one shown in point (a), deduce at which positions we can terminate the MMI. (instead of selecting a precise length, you can also define small intervals). **(5 points)**

c) Show the top view of the electric field (y component) when the X-coupler is excited from both input ports, with a phase shift of $\frac{\pi}{2}$ for Port 2. As before, plot the electric field (abs value) along the cut-lines AB and A_0B_0. Compare this result with point (b) and argue why we cannot terminate the MMI in the center. **(10 points)**
To implement a phase shift between the ports, repeat the same steps to excite both ports and press on "Simultaneous" in the "Excitation List..." window. The phase shift must be given in degrees

d) Show the top view of the electric field (y component) when the X-coupler is excited from both input ports, with a phase shift of $-\frac{\pi}{2}$ for Port 2. As before, plot the electric field (absolute value) along the cut-lines AB and A_0B_0. Comparing this result with the one in the previous points, determine the proper length of the MMI. **(10 points)**

e) Using the length extracted in the previous point, simulate the definitive X-coupler when it is excited only by the fundamental mode in port 1. Place here the top view of the electric field (y component) and the S parameters. Comment on the result. **(5 points)**

Solution:

a) The electric field is shown in Fig. 11. The results resemble the field distribution in the Y splitter.

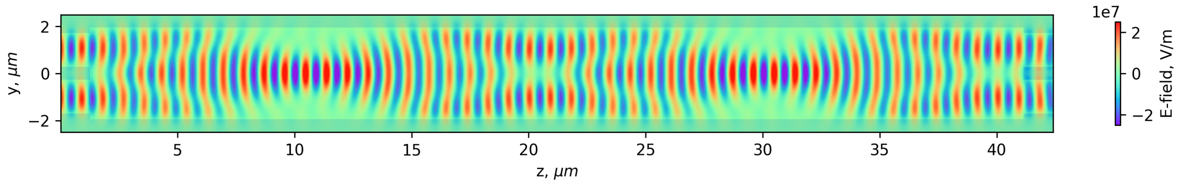

Figure 11: Y component of the electric field viewed from the top

b) The solutions for b are shown in Fig. 12. We observe in the cutline that the electric field splits into two equal components around 20 and 40 microns.

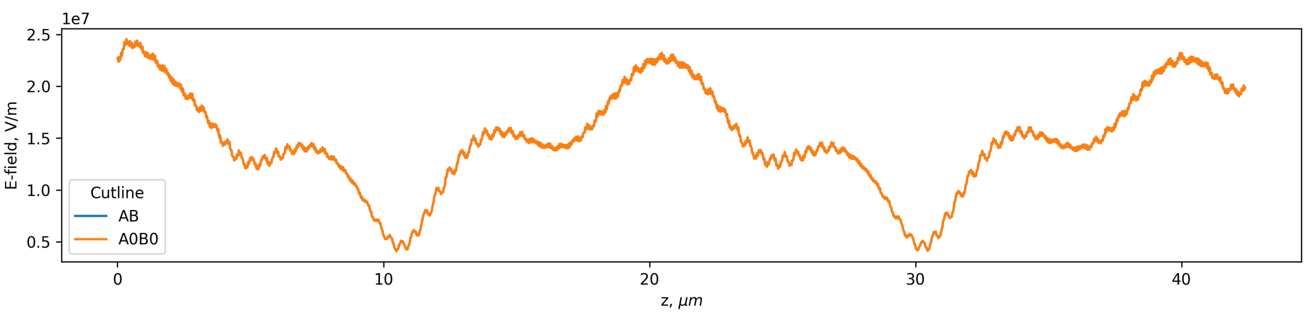

Figure 12: Electric field (abs) viewed from the top and the corresponding cutlines (AB and A_0B_0)

c) The solutions for c are shown in Fig. 13 and 14. The phase difference is evident in the blue and red colours where the ports are excited. We observe that the electric field is combined into a single output at around 40 microns.

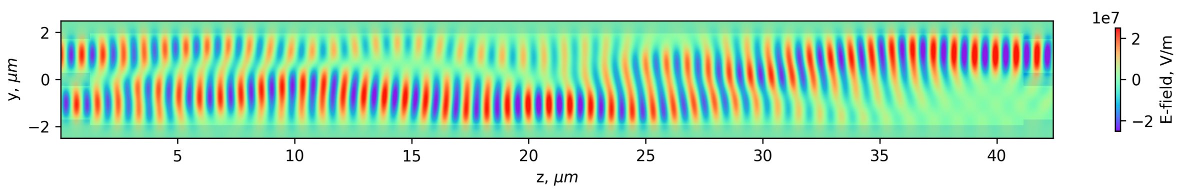

Figure 13: Electric field (Y component) viewed from the top. A phase shift of -90° is applied on the ports

d) The solutions for d are shown in Fig. 15 and 16. This result is totally analogous to the one obtained in point (c), with the only difference that the reversed phase delay in input produces a single maximum for a positive value along y. Therefore, if we select again a length around 40 um for the MMI we can combine our inputs also in the other output waveguide.

e) At this point, we can finally choose a definitive length for our interferometer. Among the values obtained in the previous points, the best choice is the one that allows the X-coupler to operate in the largest amount

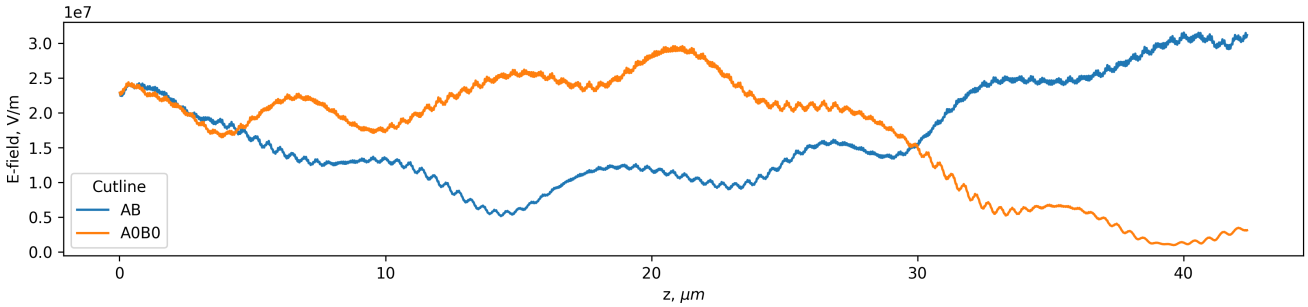

Figure 14: Electric field (abs) cutlines when phase shift of -90° is applied on the ports

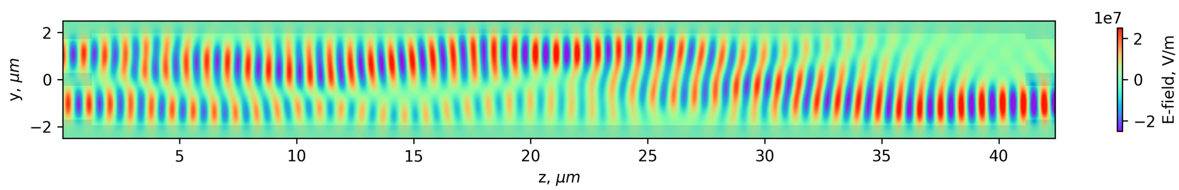

Figure 15: Electric field (Y component) viewed from the top. A phase shift of 90° is applied on the ports

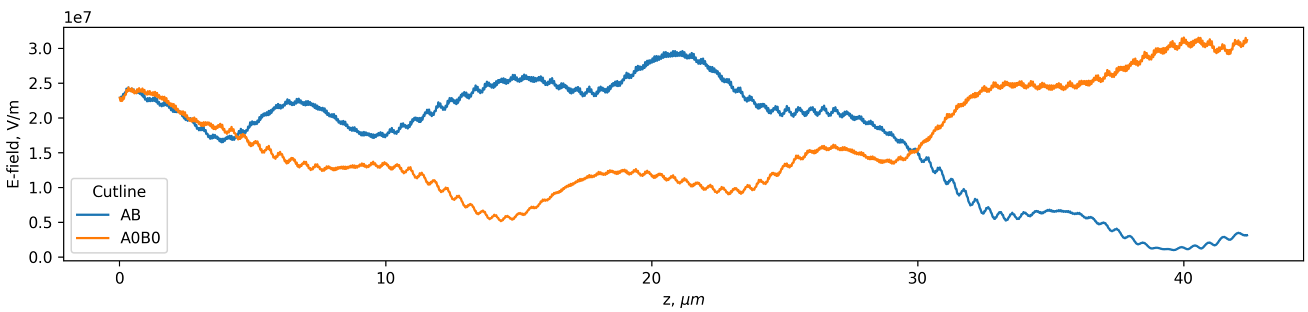

Figure 16: Electric field (abs) cutlines when phase shift of 90° is applied on the ports

of configurations, namely to enable at the same time an efficient combination of 1 or 2 inputs into 1 or 2 outputs. We can therefore choose a length of 40 um, at which we obtained the maximum coupling at points (c) and (d). The solution for e is shown in Fig. 17 and 18. We see that the X-coupler provides equal splitting when such length is chosen

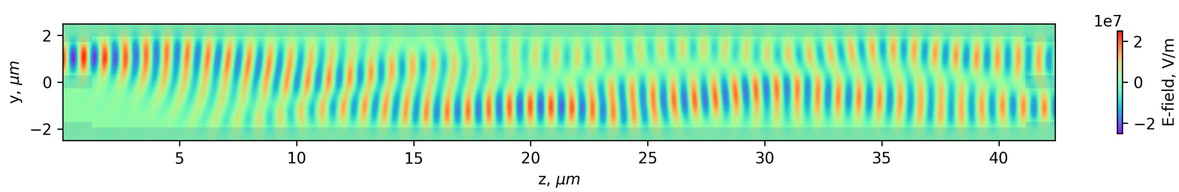

Figure 17: Electric field (Y component) viewed from the top

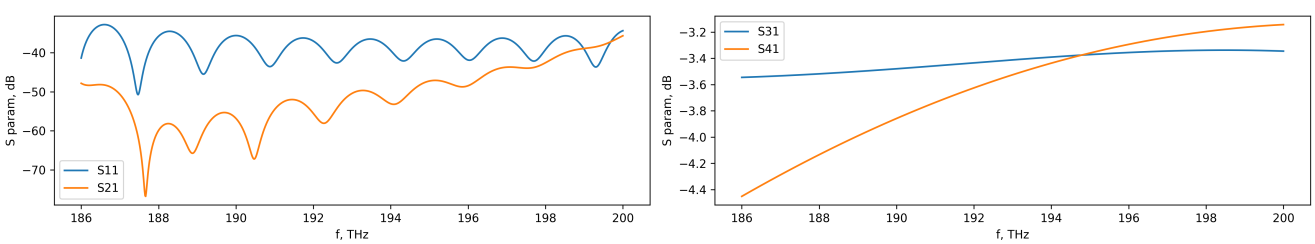

Figure 18: S-parameters